

Supplemental Material

Supplemental Methods

PCR Primers:

Acadm (mouse # Mm01323361_mH), CD36(mouse # Mm00432403_m1), Cpt1a (mouse # Mm00550448_m1), Hadh (mouse # Mm00492535_m1), Acot1 (mouse # Mm01622471_s1), PDK4 (mouse # Mm01166879_m1), Dgat1 (mouse # Mm00515643_m1), fabp1 (mouse # Mm00444340_m1), Ucp1 (mouse # Mm01244861_m1), Cidea (mouse # Mm00432554_m1), Prdm16 (mouse # Mm00712556_m1), Dio2 (mouse # Mm00515664_m1), Adrb3 (mouse # Mm02601819_g1), PPAR α (mouse # Mm00440939_m1), Atp6 (mouse # Mm03649417_g1), cox1 (mouse #Mm04225243_m1), cycs (mouse #Mm01621048_s1), Nd1 (mouse # Mm04225274_s1), Nrf1 (mouse # Mm00447998_m1), ppargc1a (mouse # Mm01208835_m1), Tfam1 (mouse # Mm00447485_m1), Nppa (mouse # Mm01255747_g1), Ctgf (mouse # Mm01192933_g1), Postn (mouse # Mm01284913_g1), Tgfb (mouse # Mm01178820_m1), Colla1 (mouse # Mm00801666_g1), Lox (mouse # Mm00495386_m1) or glyceraldehyde-3-phosphate dehydrogenase (GAPDH, mouse #99999915_g1,) by Applied Biosystems.

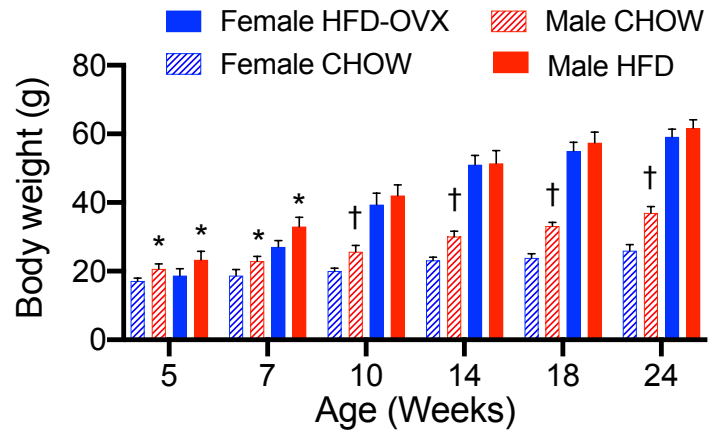
EM gold sample preparation:

NRVMs fixed in EM grade 4% paraformaldehyde, 0.1% glutaraldehyde in 80 mM phosphate buffer (Sorenson's buffer) with 3 mM magnesium chloride, pH 7.2 where then processed, with all subsequent steps performed at 4⁰C until 70% ethanol dehydration. Samples were first rinsed 3 times in buffer containing 3% sucrose, then incubated in 1.5% potassium ferrocyanide reduced 1% osmium tetroxide in 80 mM phosphate buffer, containing 3 mM magnesium chloride followed by two distilled water rinses, dehydrated in a graded series of Ethanol, followed by propylene oxide, and embedded in EPON (Ted Pella, Inc.). Plates are baked at 37⁰C for 2-3 days

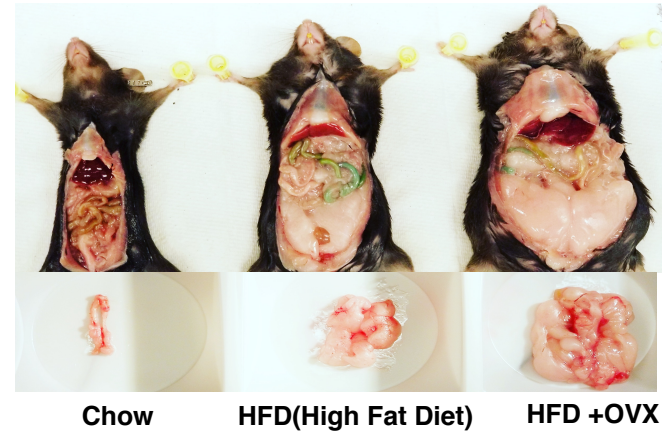
before an overnight bake at 60°C. 80-90 nm ultra-thin sections were picked up on formvar coated 200 mesh nickel grids and allowed to dry. Grids were floated on all subsequent steps. All solutions were filtered except for antibodies which were centrifuged at 13K for 5 min. Grids were wetted 3 times on D-H₂O, then placed on 3% sodium metaperiodate for 20 min. After a 15 min rinse in D-H₂O, grids were placed in 50 mM NH₄Cl in TBS for 10 min, followed by 20 min block in blocking solution (3% normal goat serum and 3% bovine serum albumin in TBST). Antibody (anti GFP, Abcam ab6556) incubation was done at appropriate dilutions (1:100) in the same block. Antibody block (no primary) served as negative control. Incubations were carried out at 4°C overnight. Blocks were equilibrated to room temperature, grids were placed on blocking solution for 10 min, followed by a 1 min rinse in TBS. Gold conjugated secondary antibody (12nm, Colloidal gold 109-185-088, Jackson Immuno Research Labs) was diluted 1:40 in TBS and sections were incubated for 2 hrs at room temperature in a humidity chamber. After a 10 min TBS incubation followed by a quick D-H₂O rinse, grids were hard fixed in 1% glutaraldehyde in 100 mM sodium cacodylate buffer for 5 min. After a brief D-H₂O rinse, grids were stained with 2% uranyl acetate (aq.) for 20 min, rinsed again with D-H₂O; blot dried and allowed to dry overnight before viewing.

Supplemental Figures and Legends

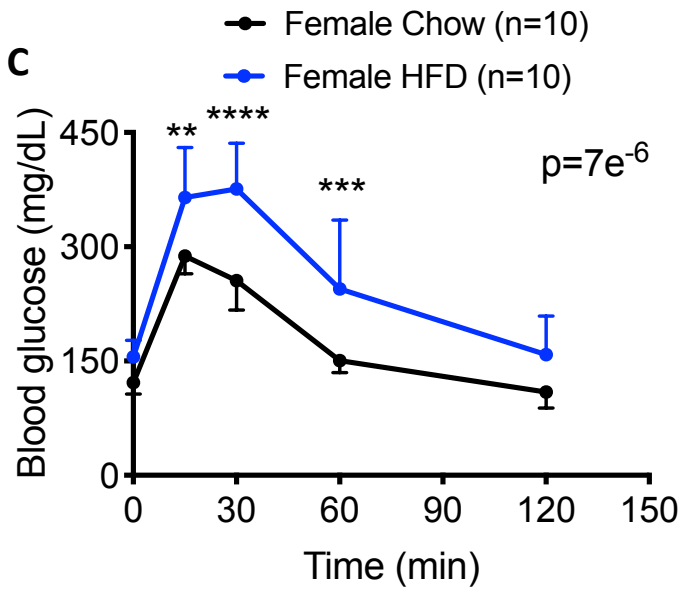
A



B



C



D

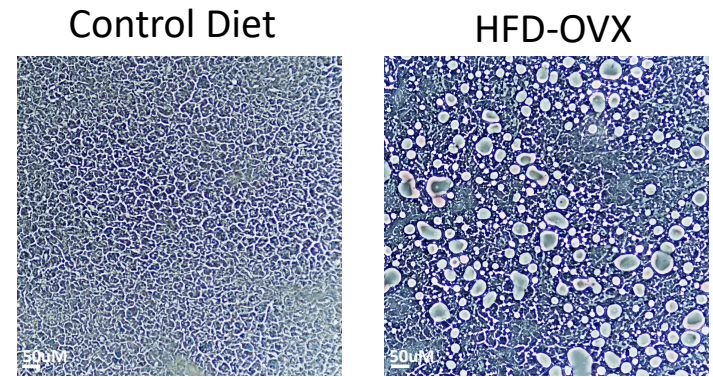


Figure S1

Supplemental Figure S1. Model of severe obesity and cardiac pressure-load (CMS) in

female C57BL6/N mice. **A)** Total body mass increase over 6-month period for ovariectomized (OVX) females and males with control or high-fat diet. N=9/group, mean \pm SD. Female weights post OVX become equal to males. * $p < 0.005$, † $p < 0.0005$ vs same diet in females. 2WANOVA, Sidak's multiple comparisons test (SMCT). **B)** Example of severe abdominal adiposity particularly in OVX females with DIO. This was representative of nearly all the mice in these cohort. **C)** Depressed glucose tolerance in OVX+HFD versus female chow-diet controls (n=10/group, 2WANOVA, SMCT; ** $p = 0.002$, *** $= 0.0001$, and **** $6.7e^{-7}$ between groups). **D)** Representative micrographics of liver in normal and DIO showing marked steatosis in OVX mice measured after 13 weeks of DIO and prior to mTAC or drug/placebo treatment (replicated x8).

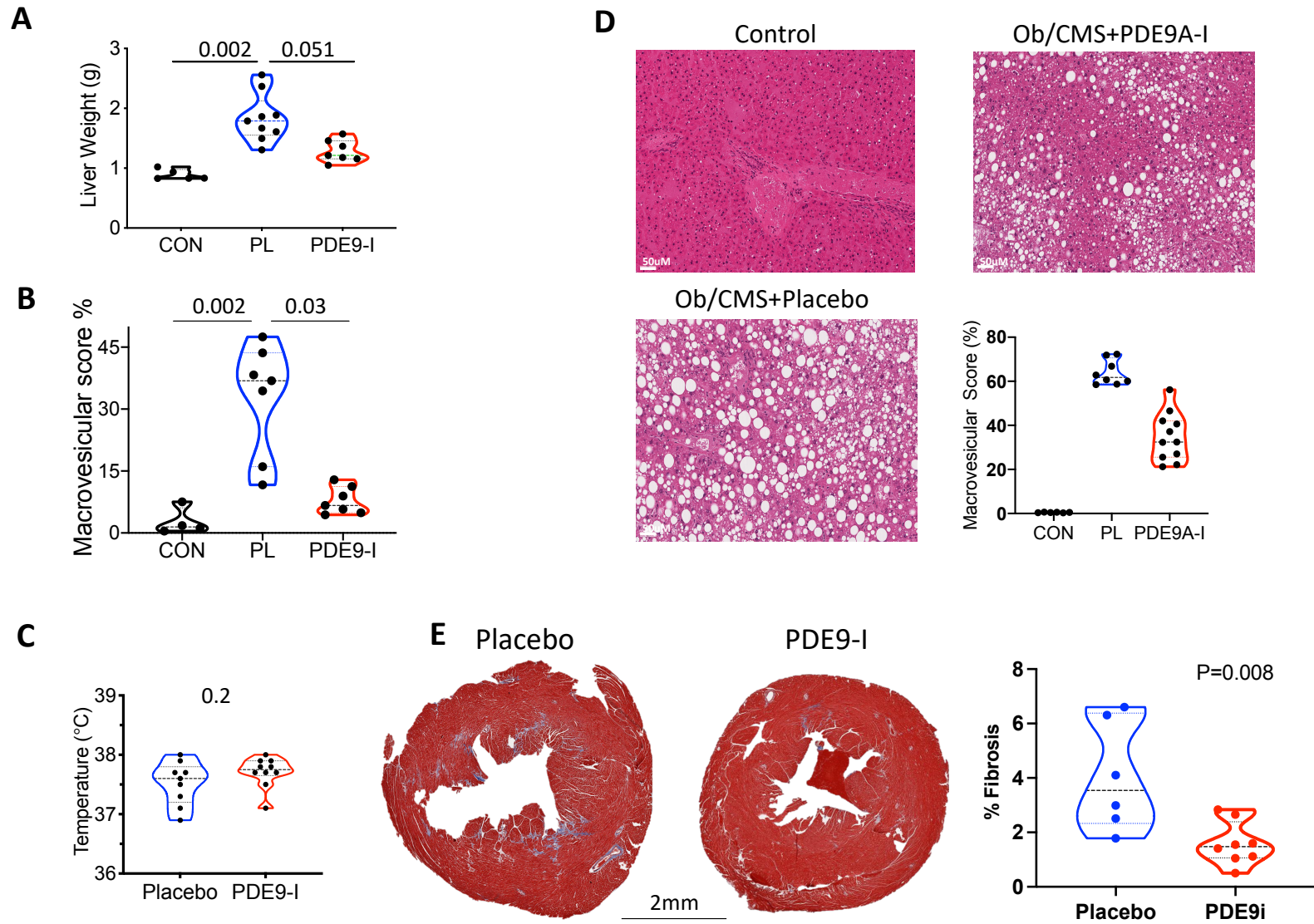


Figure S2

Supplemental Figure S2. Hepatic steatosis in OVX and male mice with ob/CMS model. A)

Quantification of hepatic mass and **B)** percent area occupied by lipid macro-vesicles in OVX

mice with DIO/mTAC model related to examples shown in Figure 1f. PL-placebo, CON- chow

diet, KW with DMCT p-values shown. **C)** Core temperature in OVX ob/CMS mice treated with

placebo versus PDE9-I. **D)** Example liver histology and summary analysis of macro-vesicular

lipid accumulation in male mice with ob/CMS model. Kruskal Wallis (KW) with Dunn's

multiple comparison test (DMCT) P values displayed. **e)** Example left ventricle cross-sectional

histology stained with Masson Trichrome stain from OVX-DIO/mTAC model with summary

results for percent fibrosis/total area for placebo (n=6) versus PDE9-I (n=8) treated mice. P value

from Mann Whitney (MW) test. As with all violin plots, median and quartiles are shown.

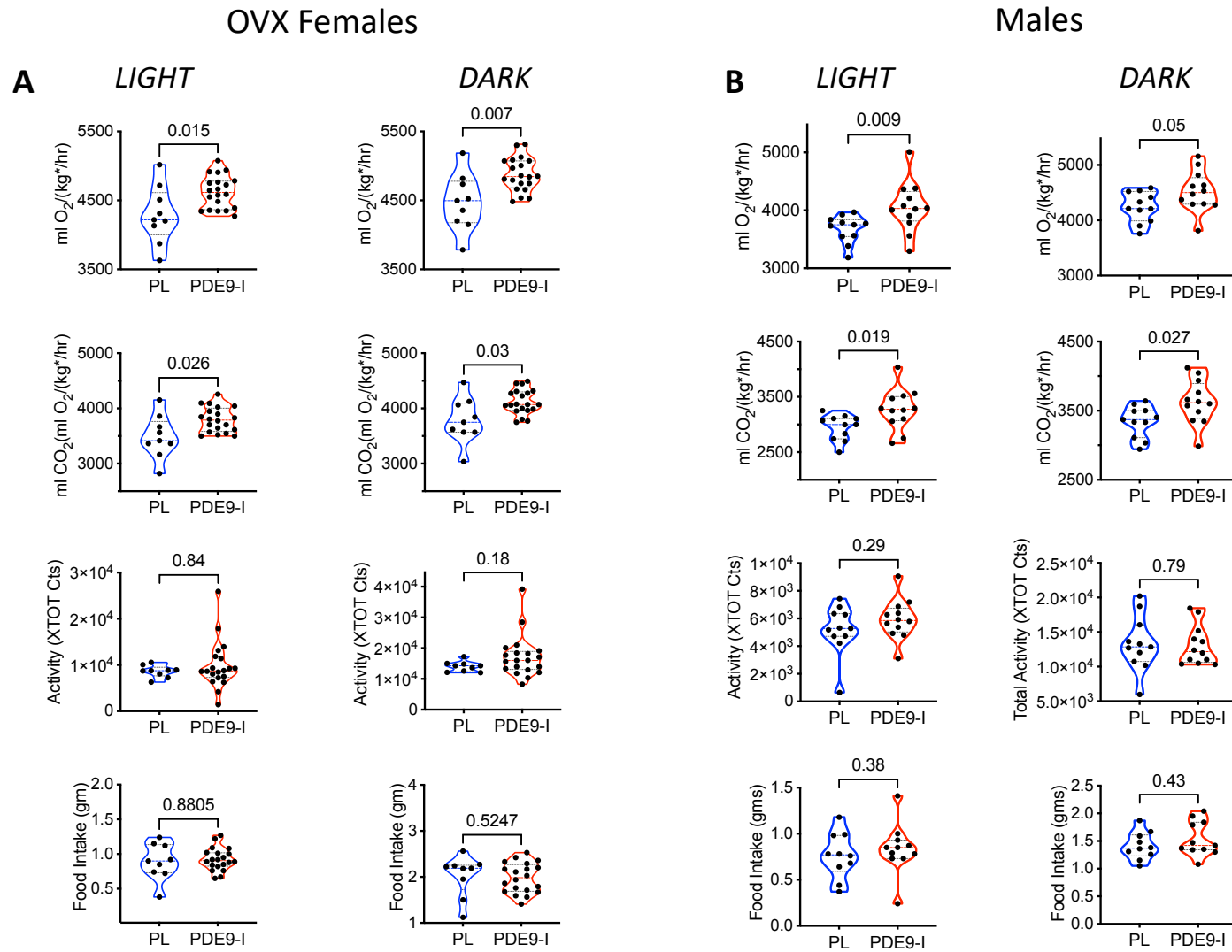


Figure S3

Supplemental Figure S3. Circadian effects of PDE9-I on today body O₂ consumption and CO₂, activity and food in OVX and Male mice with DIO/mTAC.

Each time period was 12 hours. PL – placebo. **A)** Data for OVX-female mice (n=9 Placebo, n=20 PDE9-I). **B)** data for Male mice (n=10 Placebo, n=9 PDE9-I). Activity is greater during the dark period as expected. For both groups in both time periods, PDE9-I increases O₂ consumption and CO₂ production without significantly altering activity or food intake. P values displayed are for MW test between the two treatment groups.

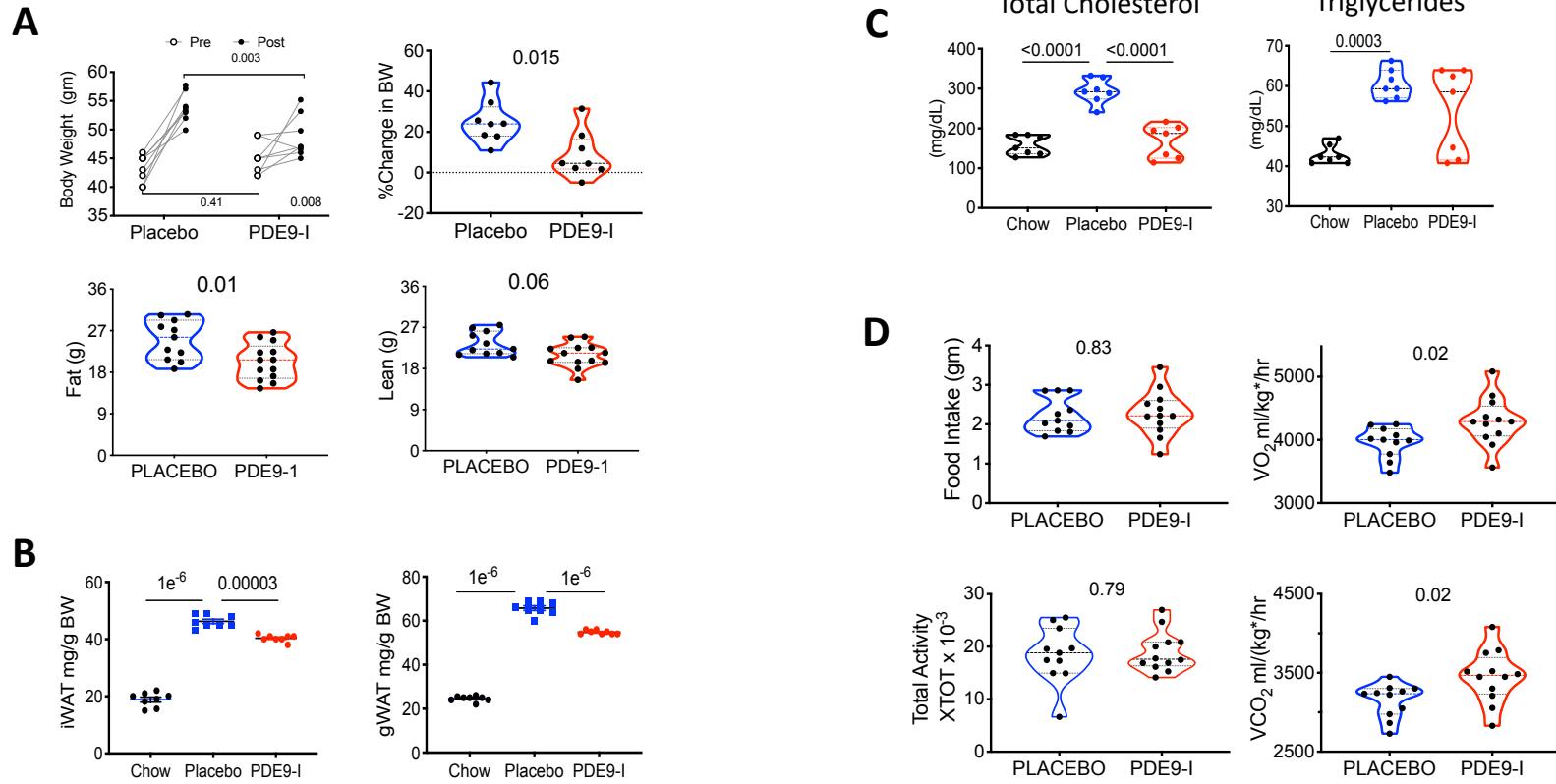
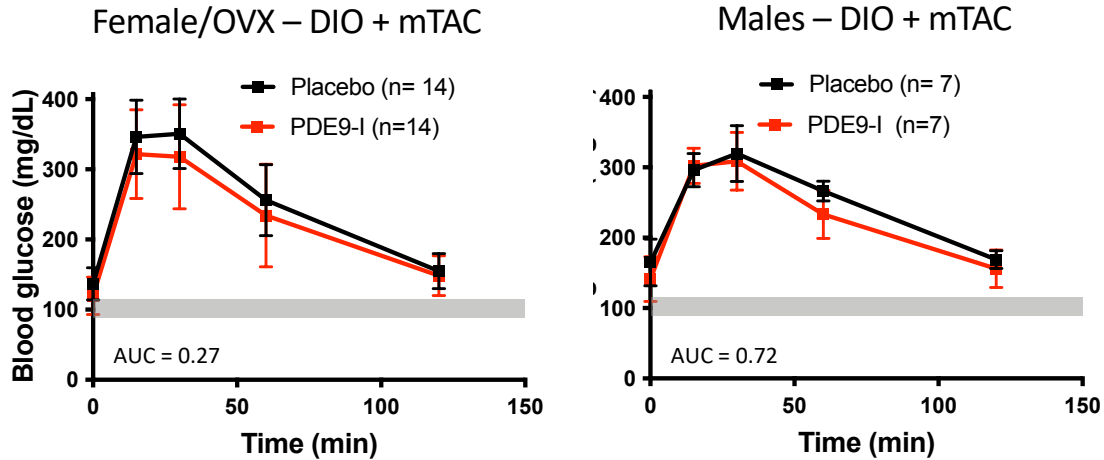


Figure S4

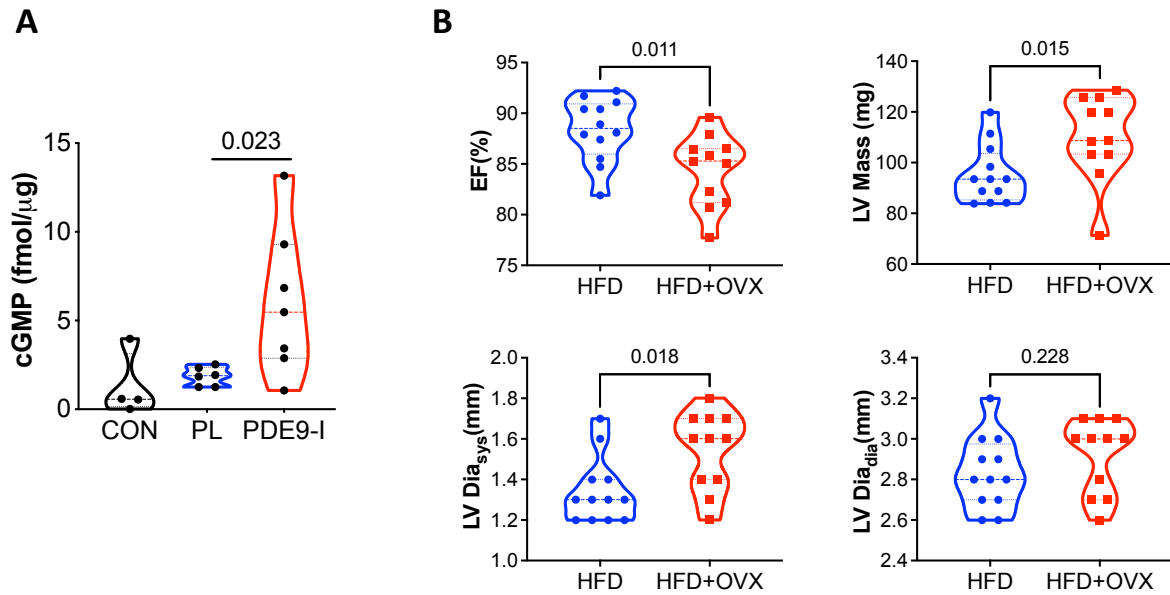
Supplemental Figure S4. PDE9-I reduces obesity and improves metabolic profile in

ob/CMS male mice. A) Total body weight before and after treatment in placebo vs PDE9-I treatment groups. (n=8, 2WANOVA, SMCT); percent change from same data, MW; MR-derived total body fat and lean mass for both groups (n=11/13, MW) **B)** iWAT and gWAT from males in both treatment arms. (n=8/group, 1WANOVA, Tukey multiple comparisons test (TMCT). **C)** End-of study serum cholesterol and triglycerides (n=7/group, 1WANOVA, TMCT). **D)** Indirect calorimetry results from same experiment (n=11/12 per group, unpaired t-test). $kg^* = (\text{lean mass} + \text{fat mass} * 0.2)$.



Supplemental Figure S5. Impact of PDE9-I on glucose tolerance test.

Glucose tolerance tests in DIO + mTAC mice from OVX and male groups treated with placebo (vehicle) versus PDE9-I. Data are mean \pm SD. Each data set is analyzed by repeated measures mixed effects model: effect of time, drug, and their interaction were: OVX: $P < 10^{-11}$, 0.2, 0.57 and Male: $P < 10^{-11}$, 0.15, 0.37.



Supplemental Figure S6. PDE9-I increases myocardial cGMP. Effect of OVX on resting

heart function and size. A) . A) Myocardial cGMP assessed in OVX mice on chow (CON) or

with ob/CMS model treated with placebo (PL) or PDE9-I. KW, P-value from DMCT. **B) M-**

mode derived left ventricular ejection fraction (EF), and end-systolic (LV Dia_{sys}) and end-

diastolic (LV Dia_{dia}) dimensions, and estimated wall mass. In mice with DIO, OVX resulted in a

slight but significant decline in EF with increased end-systolic dimensions, and greater LV mass.

This accompanied greater obesity. P values are from MW test.

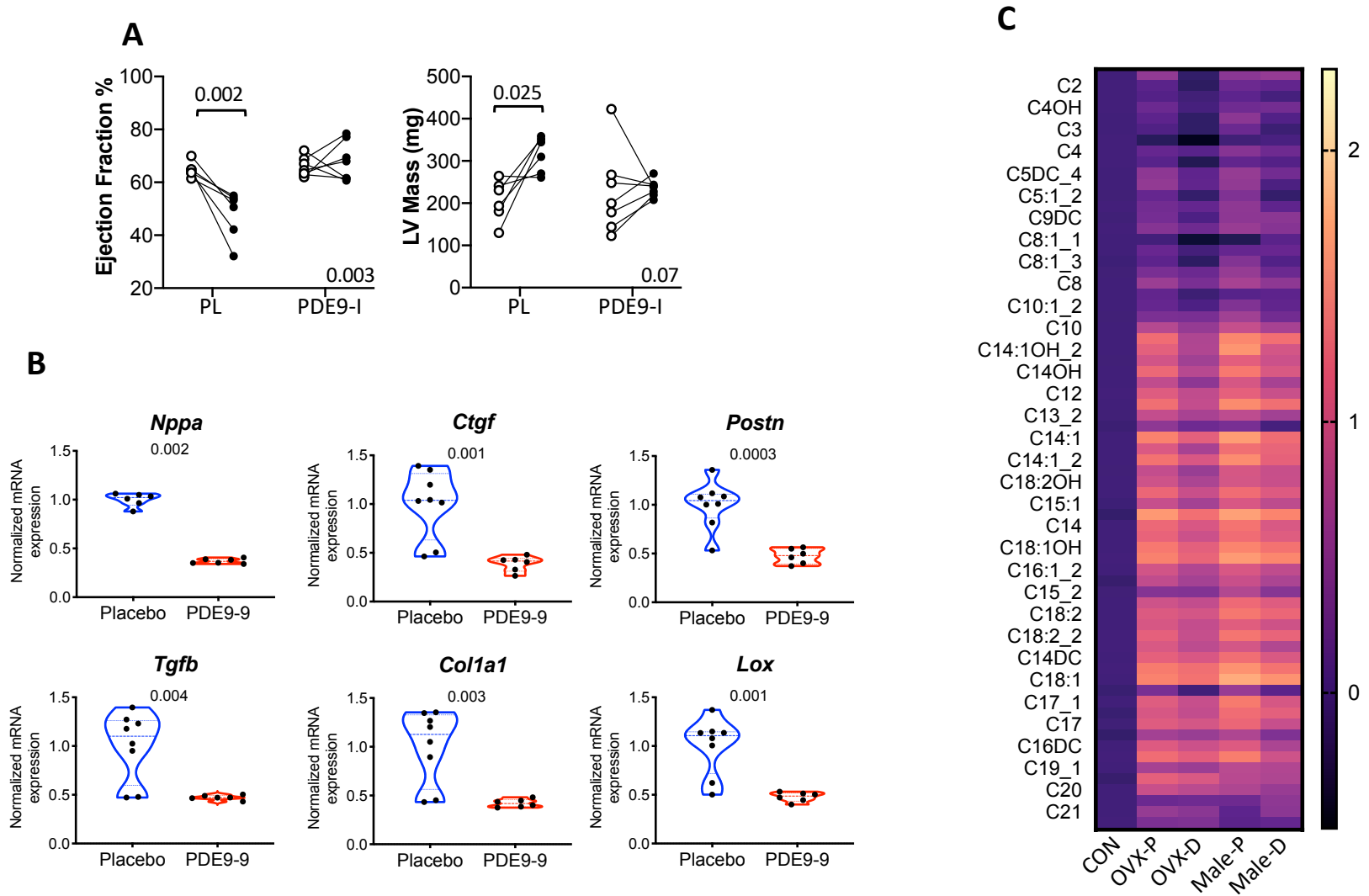


Figure S7

Supplemental Figure S7. PDE9-I improves male ob/CMS mouse cardiac function, pathological hypertrophic/fibrotic molecular signature, and fat metabolome A)

Echocardiography for ejection fraction and LV mass in male ob/CMS mice treated with placebo or PDE9-I. (n=6,7/group, 2WANOVA P-value for interaction at lower right, upper P values for Tukey multiple comparisons test. **B)** Quantitative PCR analysis of mRNA for hypertrophic and pro-fibrotic signaling genes in myocardium of males at termination of the same protocol.

Abbreviations as provided in Figure 2C legend. KW P-values displayed for each gene. **C)** Heat map (log transformed) for acyl-carnitine metabolites in myocardium of mice fed normal diet (CON) or OVX or Males with DIO/mTAC CMS treated with placebo (PL) or PDE9-I (n=5/group). Statistical analysis performed using 2-step Benjamini, Krieger, Yekutieli procedure for multiple Mann Whitney comparisons, 1% FDR. All analytes in both OVX and Males were significantly increased from non-obese control levels at adjusted Q value <0.002. 89% and 85% of all analytes were significantly reduced (Adjusted Q<0.05, most Q=0.01) by PDE9-I treatment versus placebo in OVX and Males, respectively. Decreases were distributed throughout the broad range of FA but most notable in long-chain FA.

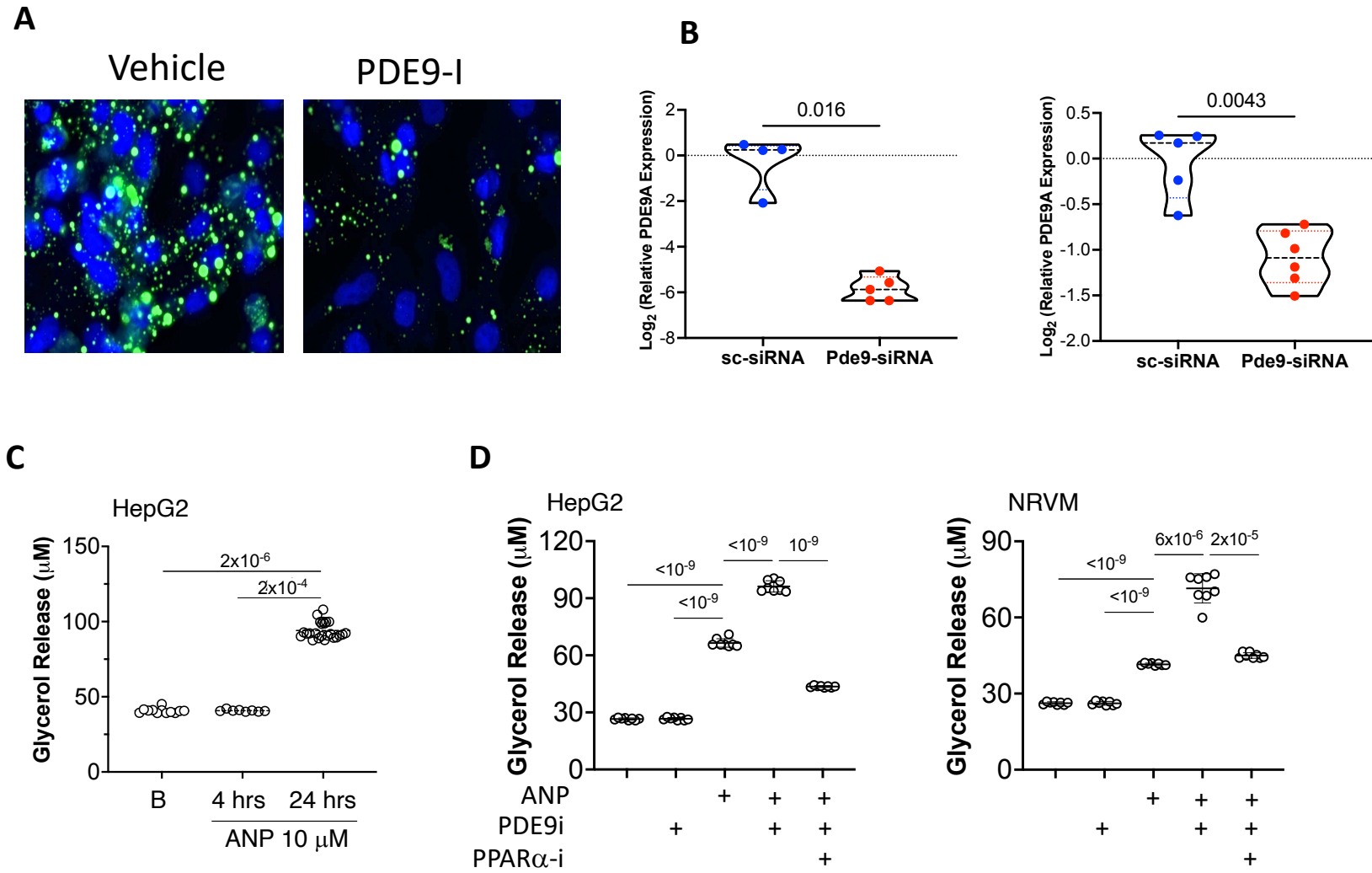
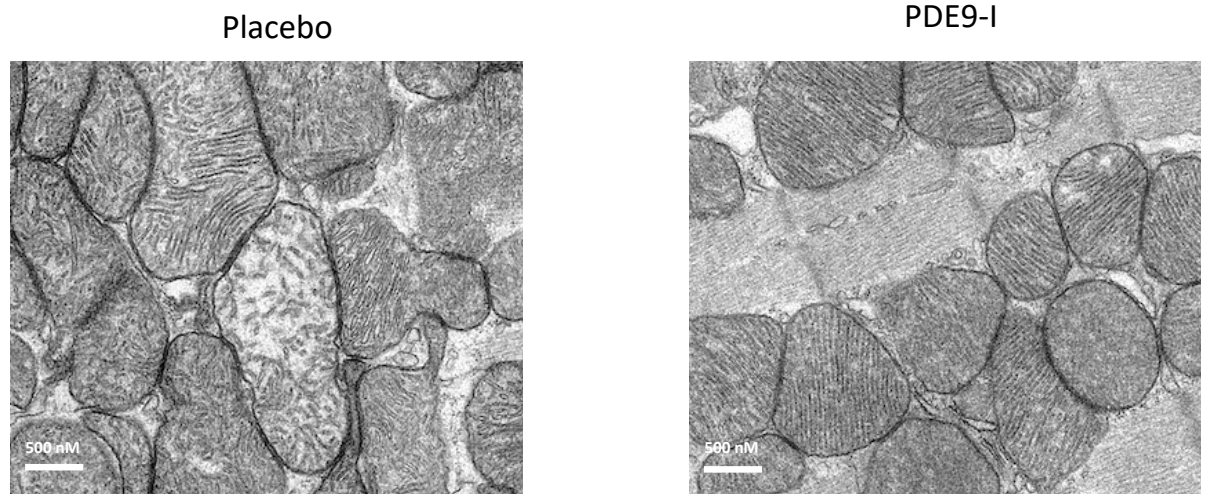


Figure S8

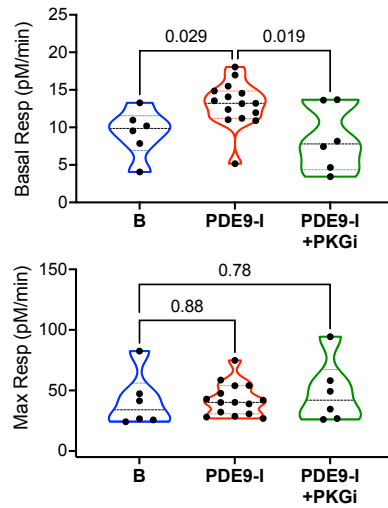
Supplemental Figure S8. PDE9-I stimulates lipolysis in cardiomyocytes and hepatic

HepG2 cells. **A)** Cardiomyocytes were loaded with 5 μ M BODIPY 493/503 to fluorescently label lipid macro droplets (green), nuclei are stained with DAPI (blue); (x3 replicates). Cells were fed a fatty acid mixture described in Methods and then incubated with vehicle or PDE9-I (PF-7493) for 24 hours prior to imaging. **B)** Result of PDE9a targeted siRNA versus scrambled (Scr) control in reducing PDE9a gene expression in human cultured adipocytes (left) and NRVM (right). **C)** Glycerol release at baseline (B, n=8), and after 4 hrs (n=8) or 24 hrs (n=24) ANP exposure in adipocytes. Analysis by KW test, P values DMCT shown. **D)** Lipolysis assessed by stimulated glycerol release in HepG2 cells or cardiomyocytes (NRVM) treated with ANP for 24 hours \pm PDE9-I. PDE9-I (PF-7493, 5 μ M) stimulated lipolysis in the presence of ANP in both cell types, but this was blunted by concomitant PPAR α inhibition. N=8/group; Welch ANOVA with Dunnet's T3 multiple comparisons test results displayed.

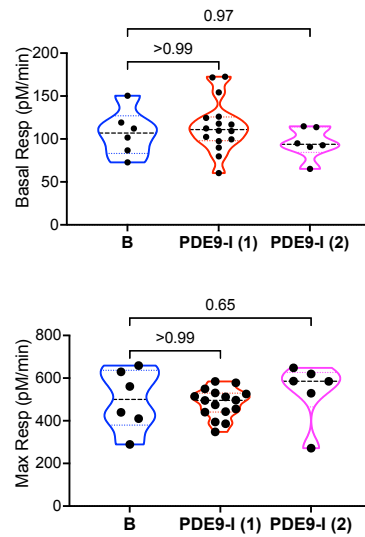


Supplemental Figure S9. Impact of PDE9-I on mitochondrial volume density and myocardial lipid accumulation. Example EM images of myocardium from male DIO/mTAC mice treated with either therapy. Upper shows typical enlarged mitochondria with reduced density observed in the placebo group. (Replicated x 4 for each group).

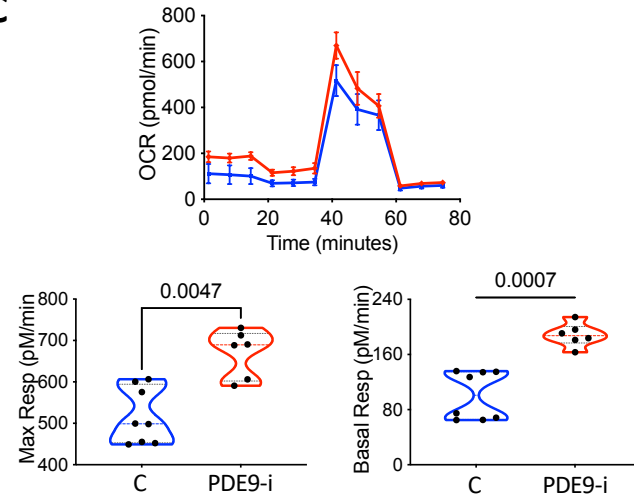
A



B



C



D

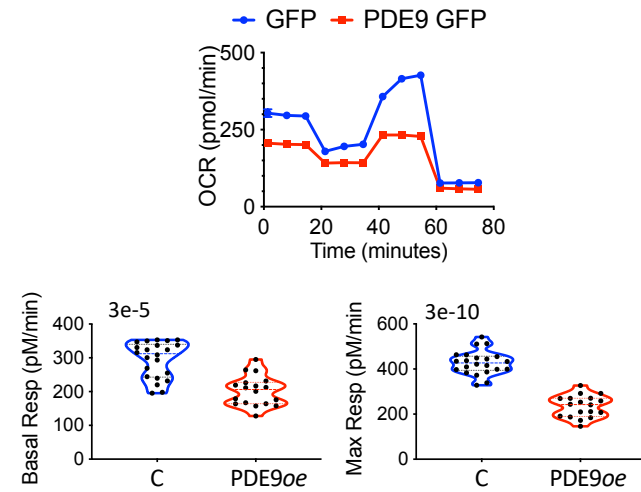


Figure S10

Supplemental Figure S10. Acute PDE9-I has minimal impact on mitochondrial basal or maximal respiration, and chronic PDE9-I (24 hrs) stimulates while PDE9a overexpression depresses both in cardiomyocytes. **A)** Basal and maximal O₂ consumption in human adipocytes at baseline (B, n=6) and after 1-hr PDE9-I exposure without (n=14) or with (n=6) concomitant PKG inhibition (PKG-I, DT3, 1 μM). Data analyzed by KW test, with DMCT P values displayed. **B)** Similar experiment and analysis in cardiomyocytes, with two different PDE9-I: (1) PF-7943, (2) BAY 73-6691, both 5 μM for 1 hour. **C)** Mitochondrial respiration in cardiomyocytes exposed to 24 hours PDE9-I (PF-7943, 5 μM). Upper panel shows time course of protocol (c.f. Figure 5d for adipocytes), mean ±SD, n=8 control, n=6 PDE9-I. Lower panels show summary data for basal and maximal O₂ consumption, same sample size, KW test P values displayed. **D)** Oxygen consumption in myocytes pre-infected with AdV expressing *Pde9a-Gfp* or *Gfp* for 48 hrs (n=18, 24, 22 respectively; KW, DMCT p-values displayed)

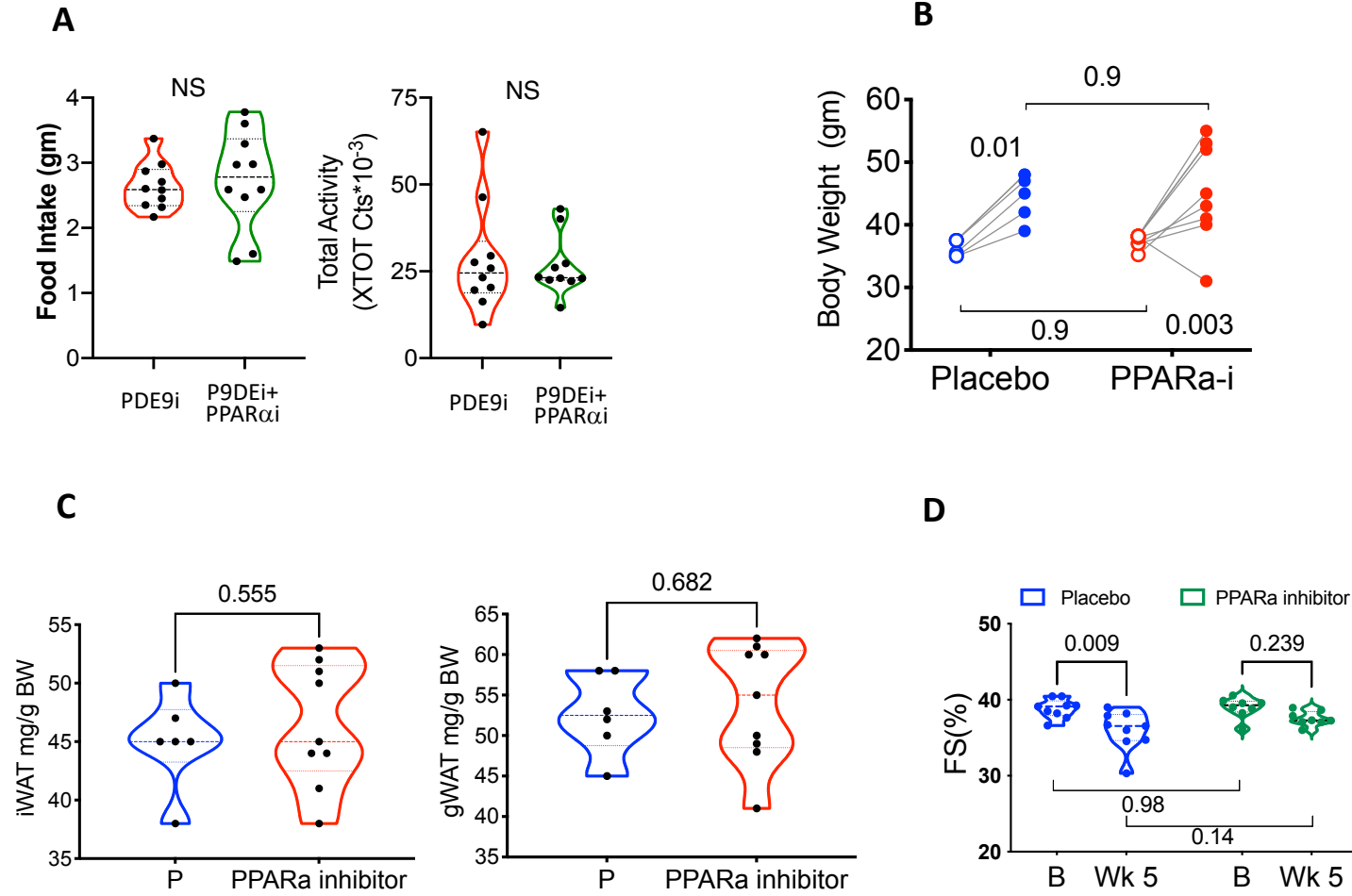


Figure S11

Supplemental Figure S11. Effect of PPAR α inhibition on food intake or activity in OVX DIO/mTAC mice; and on weight, fat mass, and left ventricular function in OVX DIO mice.

A) Food intake and activity OVX obese/CMS mice treated with either PDE9-I alone or in combination with PPAR α -I had no significant differences in daily activity or food intake. **B)** Total body weight of female OVX DIO mice without mTAC treated with placebo or PPAR α inhibitor (GW 6471). PPAR α inhibition did not significantly change the magnitude of weight gain found in both groups ($P=0.96$ for interaction term) over the 6-week period. 2WANOVA, $N=5$ placebo; 9 PPAR α -I, Sidak's multiple comparison test P values displayed for various pairs. **C)** Fat mass of iWAT and gWAT in same study testing effect of PPAR α -I alone. There was no significant difference in mass between groups. $N=6$ placebo, 9 PPAR α -I; results of MW test shown. **D)** LV percent fractional shortening (%FS) data from same experiment. There was a slight though significant decline in %FS in the placebo but not PPAR α -I group. Same statistical analysis used as in panel b, and P values from Sidak's MCT shown.

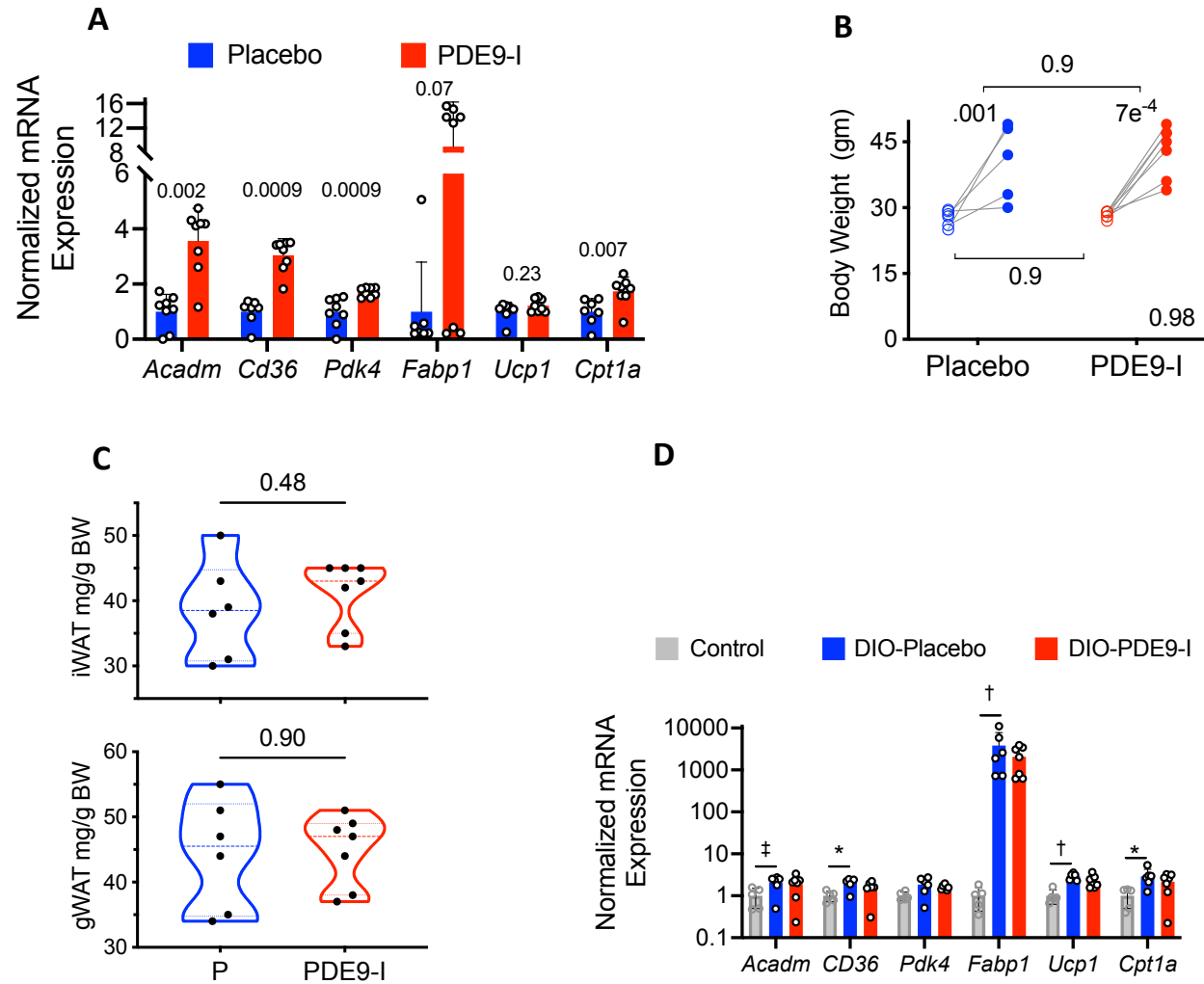


Figure 12

Supplemental Figure S12. Effect of PDE9I on PPAR α -associated mRNA abundance in BAT from male mice with DIO but without mTAC; and on weight, fat mass, and BAT expression of similar genes in non-OVX female mice with DIO and no mTAC. A)

Expression shown relative to placebo treated group (N=8/group, analysis by 2S-BKY-MW, Q values displayed. **B)** Body weight before and after 6-week treatment with placebo or PDE9-I in non-OVX DIO mice (no mTAC) shows similar weight gain. 2WANOVA, SMCT P values displayed. **C)** Weight of gWAT and iWAT are not significantly different between same treatment groups. KW P values shown. **D)** Expression of PPAR α -associated genes in non-OVX DIO without mTAC with placebo (n=6) versus PDE9-I (n=7), and non-obese controls (n=5). Data plot on log scale. While most of the genes have increased expression with DIO, there is no further change from PDE9-I. Statistical analysis as in panel **A**, Q values for control vs DIO comparison are displayed. For placebo vs PDE9-I all Q values were >0.41 .

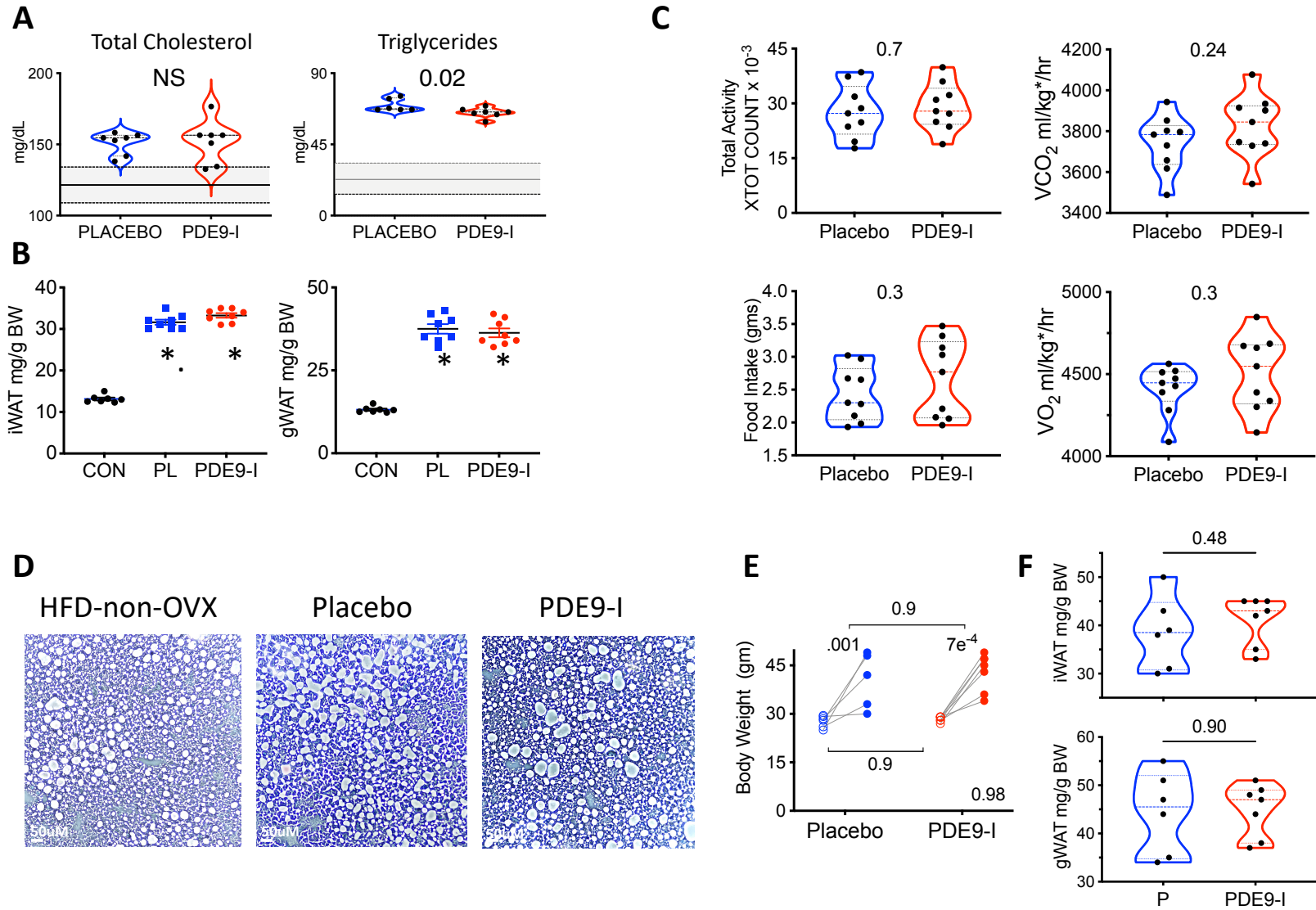


Figure S13

Supplemental Figure S13. Non-OVX females display no significant changes in serum lipids, iWAT or gWAT weight, food intake, activity, whole body metabolism, or hepatic lipid accumulation in response to PDE9-I. **A)** Non-OVX mice with DIO/mTAC model treated with placebo or PDE9-I for 8 weeks show similar plasma lipids levels. N=7/group; MW P-values shown. **B)** Both iWAT or gWAT mass increase similarly in placebo (PL, n=8) and PDE9-I (n=8) treated non-OVX over lean-controls (n=7). **C)** Activity, food intake, VO₂, and VCO₂ (latter normalized to lean + 0.2x fat mass) are similar between placebo and PDE9-I treatment (n=9/group), MW test. **D)** Lipid accumulation in the liver is similar in non-OVX in either group. Replicated n=6/group. **e)** DIO obesity without mTAC in non-OVX exhibits similar body weight changes and iWAT and gWAT mass in placebo (P) and PDE9-I groups. For weight analysis, 2WANOVA, P value to lower right is interaction term, others values for paired comparisons by SMCT.

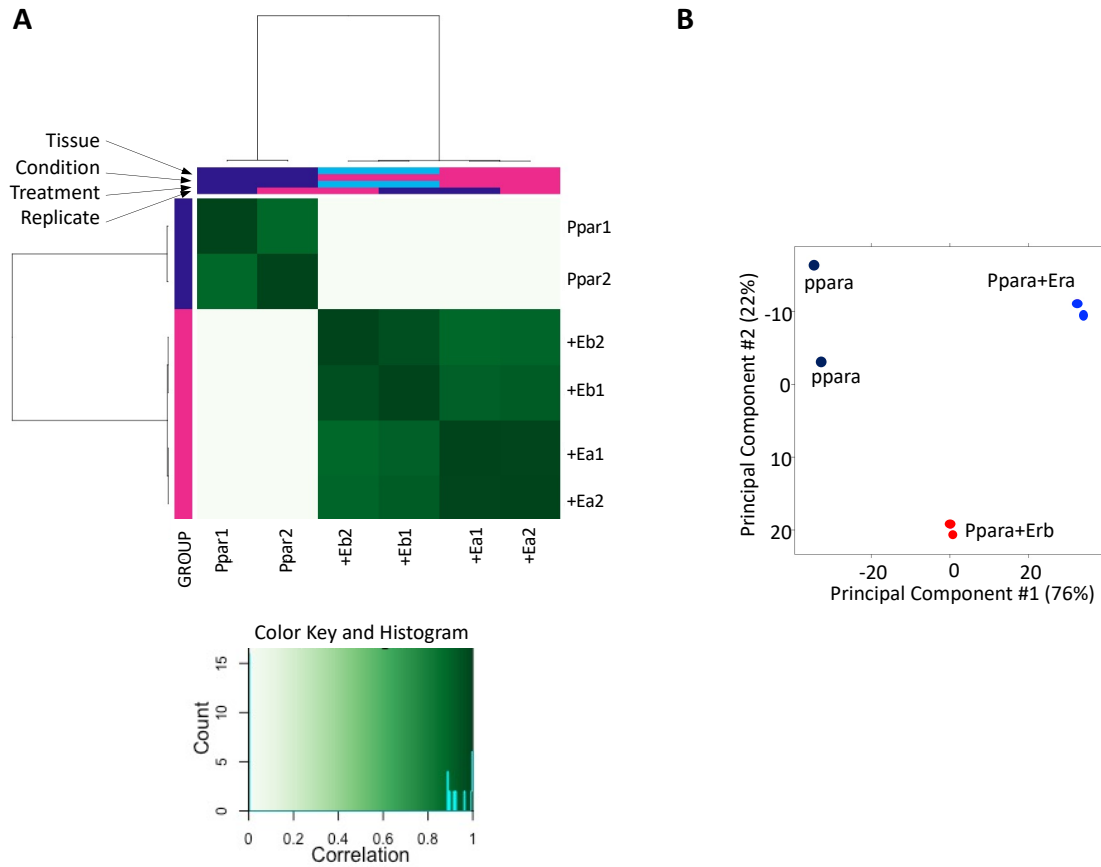
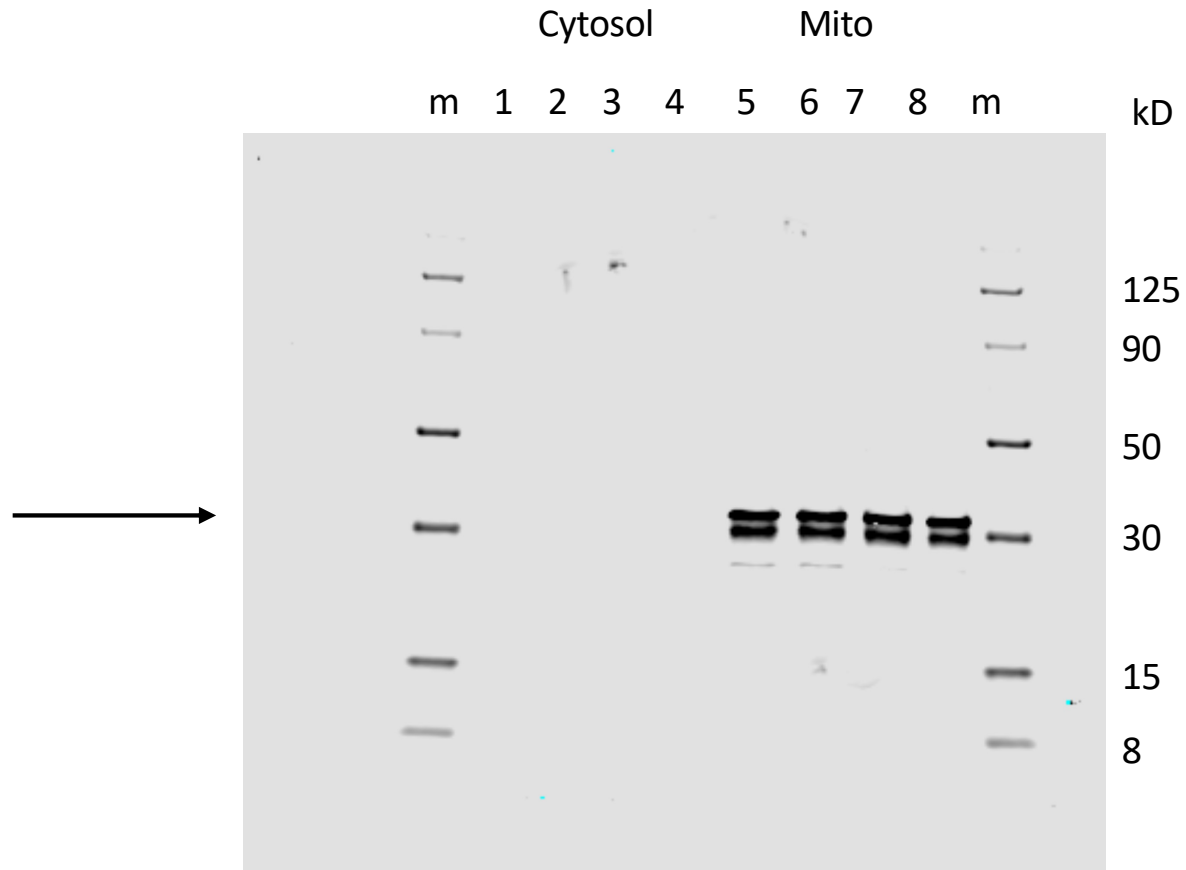


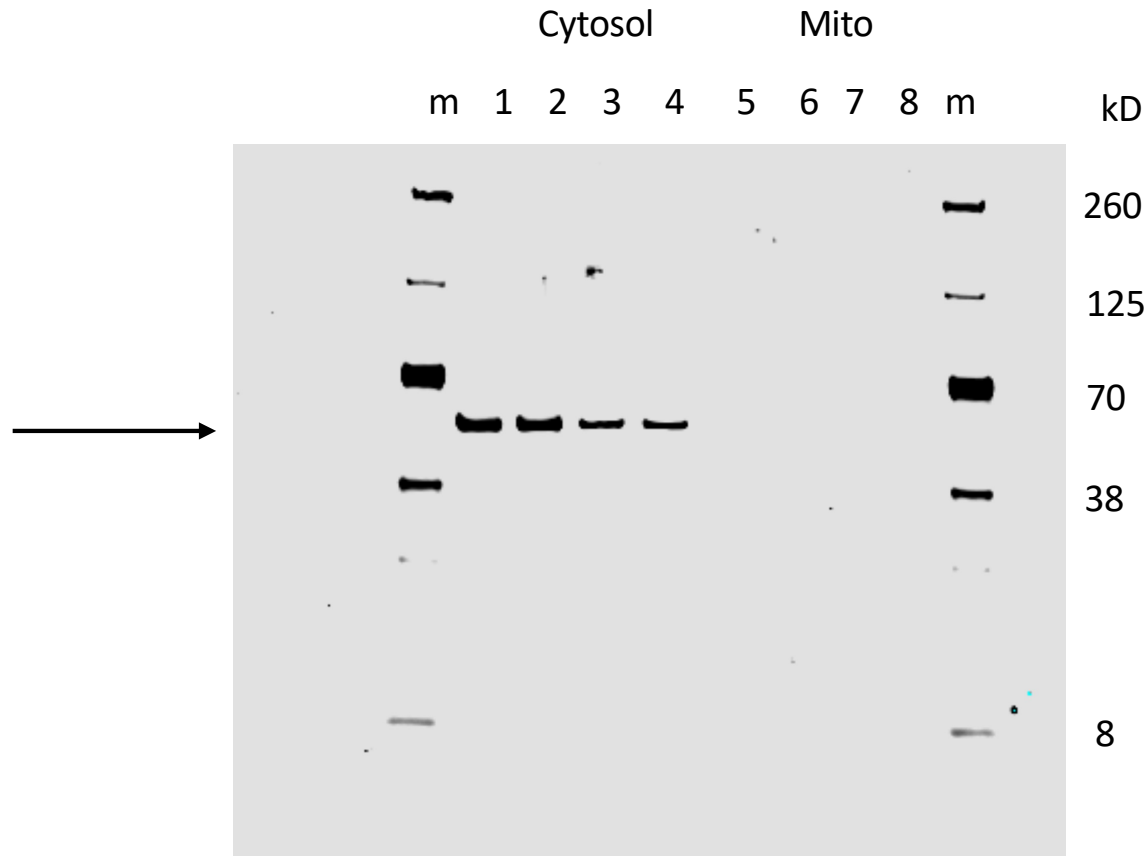
Figure S14

Supplemental Figure S14. A) Non-negative matrix factorization analysis of genes with PPAR α chromatin binding identified by ChIPSeq displays strong internal correlation of each experimental run within each experimental group (PPAR α alone, PPAR α +ET α , PPAR α +ER β). The latter cluster more closely together but quite differently from PPAR α alone. **B)** PCA analysis of same gene sets also shows consistency between experiments and marked separation between the three groups.

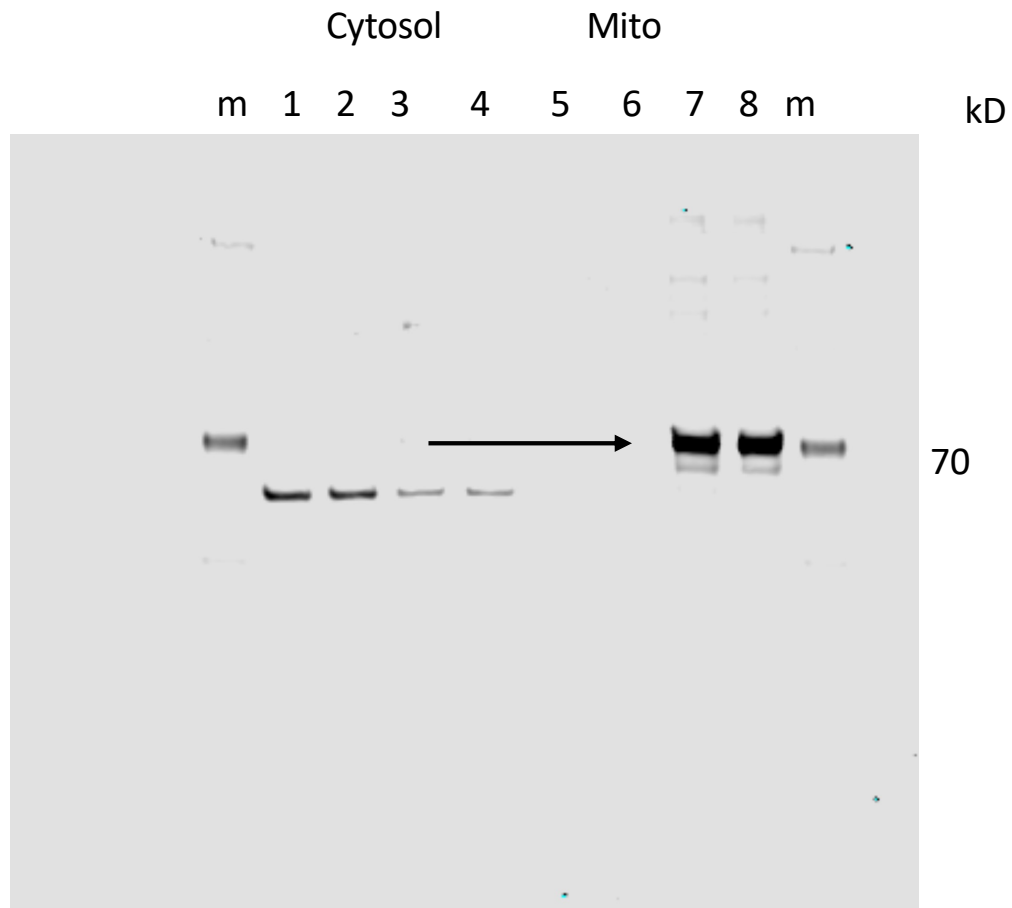
VDAC – Raw Gels



Alpha Tubulin – Raw Gels



FLAG – Raw Gel



Total Protein Stain – Raw Gels

